Reprinted from
ASLE TRANSACTIONS 6, 346-357 (1963)
Academic Press Inc.
Printed in U.S.A.

Theoretical and Experimental Investigation of Gas-Lubricated, Pivoted-Pad Journal Bearings

By E. J. GUNTER, JR.,[1] V. CASTELLI,[2] and D. D. FULLER (ASLE)[3]

This paper presents some of the theoretical predictions and experimental results for the steady-state characteristics of a gas-lubricated, pivoted-pad journal bearing of finite length. An analytical expression for the prediction of load-carrying capacity for these bearings is developed from numerical computer solutions. Sample calculations are presented to show how the theoretical data may be utilized in the design of an actual pivoted-pad bearing. Improvements over previous approximate theories are discussed.

Nomenclature

B = shoe length in the circumferential direction = $R\alpha$, inches
C = radial clearance between shoe and shaft = $R_{\text{shoe}} - R_{\text{shaft}}$, inches
C_L = load coefficient = $W/(P_a RL)$, dimensionless
C' = pivot circle radial clearance = $R_{\text{pivot}} - R_{\text{shaft}}$, inches
e = eccentricity between shoe and shaft center, inches
e' = eccentricity between pivot circle center and shaft center, inches
f_a = side leakage factor, dimensionless
h_m = minimum film thickness, inches
h_{pi} = pivot film thickness for shoe i, i = 1,2,3, inches
h_L = leading edge film thickness, inches
h_T = trailing edge film thickness, inches
H = dimensionless film thickness = h/c
L = shoe width, inches
L/B = aspect ratio, dimensionless
N = rpm
P_a = ambient pressure, psi
p = local lubricant pressure, psi
$P = p/P_a$ = dimensionless pressure
P_i = i'th pivot location; i = 1,2,3
R = shaft radius
W = shoe load capacity, pounds
W_i = load on i'th shoe; i = 1,2,3, pounds
W_s = shaft load
O_p = pivot circle center
O_j = journal center
x = horizontal displacement of the journal center from the pivot circle center
y = vertical displacement of the journal center from the pivot circle center, inches
$|n_x$, $|n_y$ = orthogonal cartesian unit vectors
$|n_i$ = unit vector set directed from O_p to P_i ; i = 1,2,3
$|r_i$ = unit vector set directed from O_j to P_i ; i = 1,2,3
α = shoe arc length, degrees
β = pivot location, degrees
ε = eccentricity ratio of shoe and shaft = e/C, dimensionless
ε' = eccentricity ratio of pivot circle and shaft e'/C', dimensionless
η = dimensionless axial coordinate
Λ = bearing compressibility parameter, dimensionless
$$= \frac{6\mu\omega}{P_a}\left(\frac{R}{C}\right)^2$$
μ = viscosity, lb sec/in^2
ξ = angle between line of centers and shoe leading edge, degrees
ϕ = angle between shoe leading edge and pivot location, degrees
ϕ/α = dimensionless pivot location
θ' = attitude angle of journal center with respect to pivot circle center, degrees
θ = angular coordinate, degrees
ω = angular velocity, rad/sec

Contributed by the ASLE Technical Committee on Bearings and Bearing Lubrication and presented at the Annual Meeting of the American Society of Lubrication Engineers held in New York, April, 1963.

[1] Research Engineer, Friction and Lubrication Laboratory, The Franklin Institute Laboratories, Philadelphia 3, Pennsylvania.

[2] Assistant Professor, Department of Mechanical Engineering, Columbia University, New York.

[3] Professor, Department of Mechanical Engineering, Columbia University, New York.

Introduction

In recent years considerable interest has been devoted to the development of design criteria for gas-lubricated bearings appropriate for high-speed rotating machinery. The

numerous advantages of gas bearings are widely known (*1*, *2*) and need not be discussed here. While many of the associated design problems have been successfully solved or circumvented, the extreme susceptibility of gas bearings to the phenomenon of self-excited half-frequency whirl instability under the conditions of high speed and light load has limited the application of the more conventional bearing configurations. On the basis of experimental (*3*) and approximate analytical results (*4*), the tilting-pad bearing configuration has demonstrated favorable stability characteristics. This feature, together with the desirable characteristic of self-alignment, suggested that detailed investigation of this type of bearing might prove to be very worthwhile.

Until now, the best available design technique for tilting-pad gas bearings was to treat the bearing as a flat inclined slider. Such a technique was the basis of the early analysis performed on pivoted-pad gas bearings by Snell (*3*), who utilized the work of Muskat *et al.* (*5*), and of Raimondi and Boyd (*6*). This technique consists of replacing the sinusoidal film distribution due to shoe curvature, with a linear function and then considering that the lubricating film is incompressible. This leads to considerable error in the prediction of the minimum film thickness and the selection of the optimum pivot location at high speeds and high loads due to the neglect of compressibility and shoe curvature.

A computer program for the tilting-pad bearing has been developed by Castelli and Stevenson (*7*) which includes shoe curvature and compressibility of the gaseous lubricant. The present paper will compare the results of the computer solution to those obtained by using the flat slider and the assumption of an incompressible lubricant. Experimental verification of theoretical predictions for the static-load case is provided by data obtained from a pivoted-pad research rig developed and operated at the authors' laboratories (*8a*, *b*, and *c*).

Bearing geometry

A schematic representation of a pivoted-pad journal bearing with three pads is shown in Fig. 1. For the purpose of analysis, the pivot points of each pad are taken to be located on the pad surface. These pivot points are also located on a circle, called the "pivot circle," of radius $R + C'$, where R is the radius of the shaft and C' is the radial clearance of the pivot circle.

The pivot circle clearance C' is an important design parameter and may be expressed in terms of the film thicknesses under each pivot by means of the following relationship:

$$C' = \frac{h_{p1} + h_{p2} + 2h_{p3}\cos\beta}{2(1 + \cos\beta)} \qquad [1]$$

The shaft center eccentricity measured with respect to the pivot circle center is:

$$e' = (x^2 + y^2)^{1/2} \qquad [2]$$

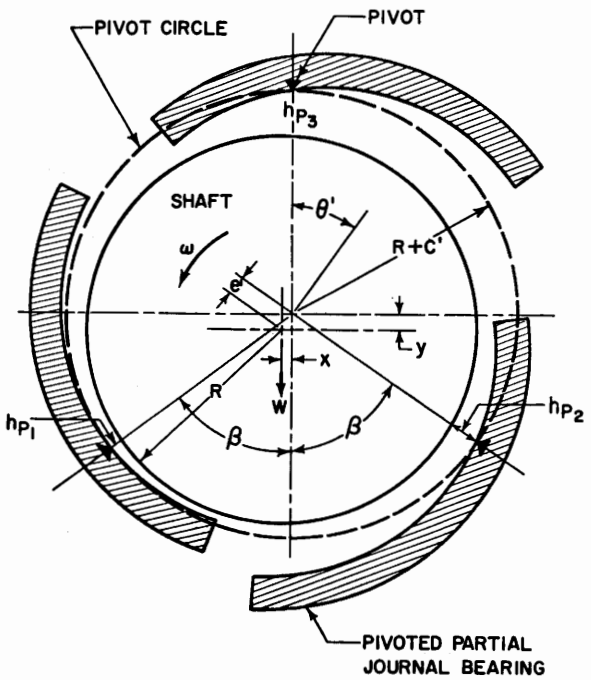

FIG. 1. Schematic diagram of a pivoted-pad bearing configuration with three shoes.

where

$$x = \frac{h_{p1} - h_{p2}}{2\sin\beta} \qquad [3]$$

and

$$y = \frac{2h_{p3} - (h_{p1} + h_{p2})}{2(1 + \cos\beta)} \qquad [4]$$

The shaft attitude angle with respect to the pivot circle and the load line is:

$$\theta' = \tan^{-1}\frac{y}{x} \qquad [5]$$

The geometry of an individual shoe and shaft is shown in Fig. 2. To describe the film distribution of a given partial-arc bearing, it is necessary to specify three quantities. These quantities consist of the clearance parameter C, which is assumed as fixed and the two variables of eccentricity ratio ε and lead angle ξ, which may assume various values. In the analysis of a composite pivoted-pad bearing configuration, the total load-carrying capacity of the bearing is obtained by computing the performance of each shoe and combining the individual results to determine the net bearing capacity. The variables of ε and ξ were used in the computer program to analyze the individual shoe characteristics.

For a multi-pad bearing, there would be a set of ε and ξ which would correspond to each shoe. As an example, for a three-pad bearing, the film thickness distribution between the i'th shoe and shaft is given by

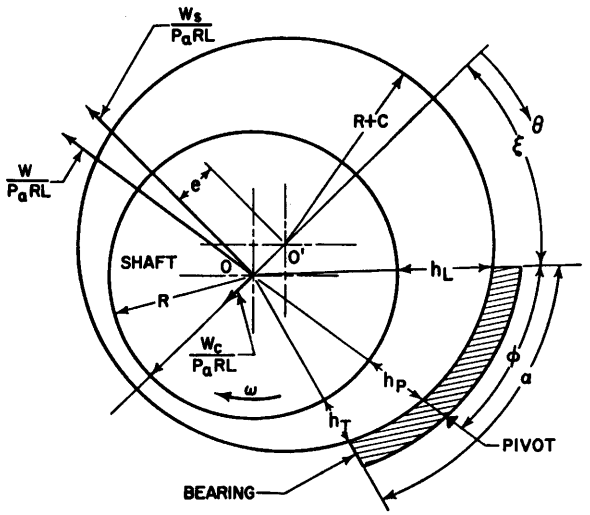

FIG. 2. Individual pivoted-pad bearing and shaft geometry

$$h_i = C[1 + \varepsilon_i \cos \theta_i]; \; i = 1,2,3 \qquad [6]$$

where C is the difference between the radii of the shoe and the shaft surfaces as manufactured, and ε_i is the eccentricity ratio $= e_i/C$.

To analyze the total bearing performance, the pivot film thickness of each pad must be specified. In this system the pivotal film thickness is given by

$$h_{pi} = C[1 + \varepsilon_i \cos (\xi_i + \phi)]; \; i = 1,2,3 \qquad [7]$$

Theoretical solution

The steady-state pressure distribution in the bearing is assumed to be governed by the two-dimensional Reynolds equation for an isothermal film (*2*) which can be expressed as

$$\frac{\partial}{\partial \theta}\left[PH^3 \frac{\partial P}{\partial \theta}\right] + \frac{R^2}{L^2}\frac{\partial}{\partial \eta}\left[PH^3 \frac{\partial P}{\partial \eta}\right] = \Lambda \frac{\partial (PH)}{\partial \theta} \qquad [8]$$

where

$\Lambda = \dfrac{6\mu\omega}{p_a}\left(\dfrac{R}{C}\right)^2 =$ bearing compressibility parameter
$\eta = Z/L =$ dimensionless axial coordinate
$P = p/P_a =$ dimensionless pressure
$H = h/C =$ dimensionless film thickness

The boundary conditions require that the dimensionless pressure assumes a value of unity at the periphery of the bearing as follows:

$$\left.\begin{aligned} P(\theta = \xi,\eta) &= P(\theta = \xi + \alpha,\eta) = 1 \\ P(\theta,\eta = \pm \tfrac{1}{2}) &= 1 \end{aligned}\right\} \qquad [9]$$

Equations [8] and [9] were expressed in finite difference form and a computer program was developed for their solution by an iterative technique (*7*). This program was used to produce field maps (to be discussed later) determining the operating characteristics for a partial bearing with an arc of 94.5° and a shoe aspect ratio of $L/B = 1$.

From Fig. 1 it is evident that, if the pads are symmetrically located with respect to the load line, they will each have a maximum arc length equal to 2β. The optimum value of the angle β and consequently of the angular extent of the bearing pads is obtained as a compromise between load-carrying capacity and resulting load on an individual shoe or pad.

The average load per bottom shoe is given by

$$W_{1,2} = \frac{W_3 + W_s}{2 \cos \beta} \qquad [10]$$

From these considerations an optimum value of β equal to 50° was chosen and the corresponding maximum allowable arc length of 100° was reduced to 94.5° for practical design reasons.

Figure 3 represents a typical computer field map for the partial bearing under consideration for a particular value of the parameter $\Lambda = 3.5$. (This corresponds to a shaft rotational speed of approximately 18,000 rpm, which is the design point for the experimental unit.)

For a given value of the compressibility bearing parameter Λ, a computer field map is obtained by selecting numerous combinations of shoe eccentricity ratio ε and lead angle ξ. For each set of values of ε and ξ there is obtained a corresponding dimensionless load and the position at which it acts. The location of the resultant load vector will determine the pivot position for static equilibrium. Therefore, for a pivoted-pad shoe, the performance characteristics are determined by the corresponding values located along the vertical line where ϕ/α equals a constant.

An important factor in the design of a tilting-pad bearing is the selection of the optimum pivot location. This is defined as the position for which the maximum load-carrying capacity is obtained for a prescribed minimum film thickness.

Lines of constant minimum film thickness can be plotted directly on the computer field map (Fig. 3). For example, the line $H_m = 0.40$ represents a minimum film thickness $H_m = h_m/C = 0.40$. To the right of the line $\xi = 85.5°$, the fluid film is converging, and the minimum thickness occurs at the shoe trailing edge; to the left, the film is converging-diverging and the minimum thickness occurs before the trailing edge.

From the study of flat sliders with incompressible lubrication, it is seen that the optimum pivot location is independent of load, but varies with the aspect ratio of the shoe ranging from $0.60B$ for an aspect ratio of unity to $0.579B$ for an infinitely wide bearing (*6*) (Fig. 4). From the computer field map of Fig. 3 for the compressible case, it can be seen that the optimum pivot location for a shoe with aspect ratio of 1.0 is not constant

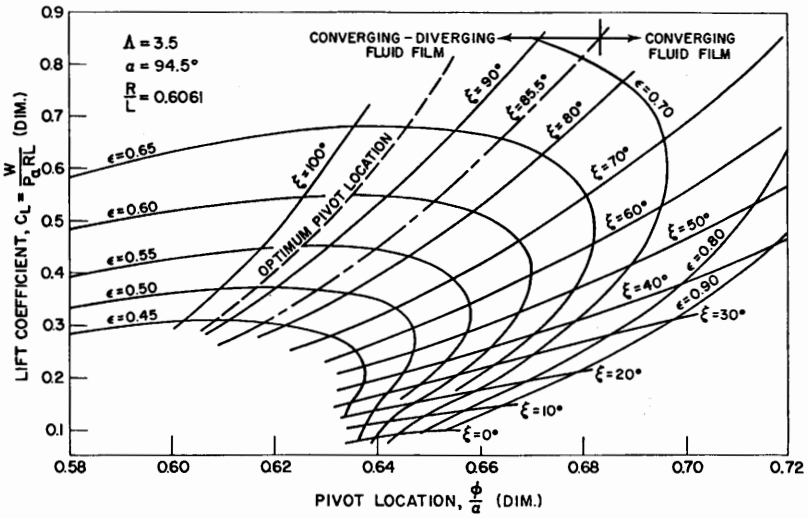

FIG. 3. Theoretical performance of a partial journal bearing for $\Lambda = 3.5$

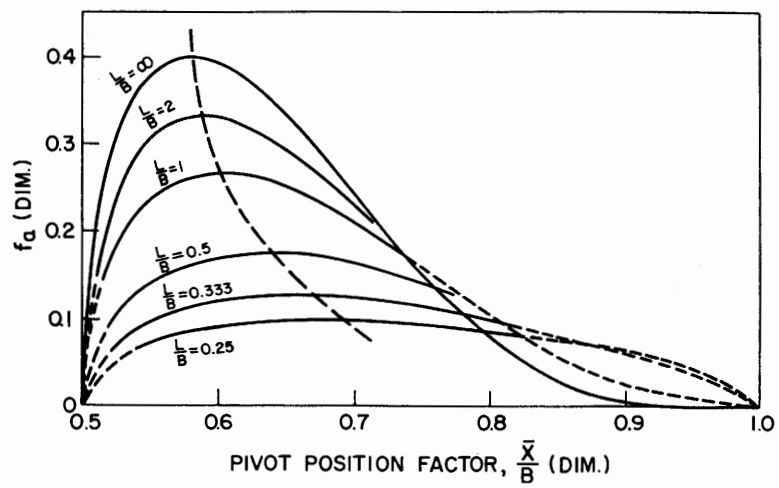

FIG. 4. Theoretical performance of a flat slider with incompressible lubricant

but varies with load and speed and ranges from 0.62 to 0.64. With this partial bearing using a compressible lubricant, an increase in load causes the optimum pivot position to move closer to the trailing edge. However, for very light shoe loads the effect of compressibility becomes negligible and the optimum pivot position approaches $0.60B$, the value predicted for bearings with incompressible lubricants.

Since the choice of an optimum pivot location is dependent on both load and speed, it should be selected to correspond to the design conditions. Examination of the slope of the minimum film thickness curves reveals, however, that the magnitude of the minimum film thickness is fortunately not sensitive to small deviations in pivot location.

Results from computer field maps for values of Λ ranging from 1.5 to 4.0 and $\phi/\alpha = \frac{2}{3}$ were used to develop the theoretical load deflection curves of Fig. 5. (The pivot location of the experimental shoes was also at $\phi/\alpha = \frac{2}{3}$.) The linearity of these curves on a logarithmic

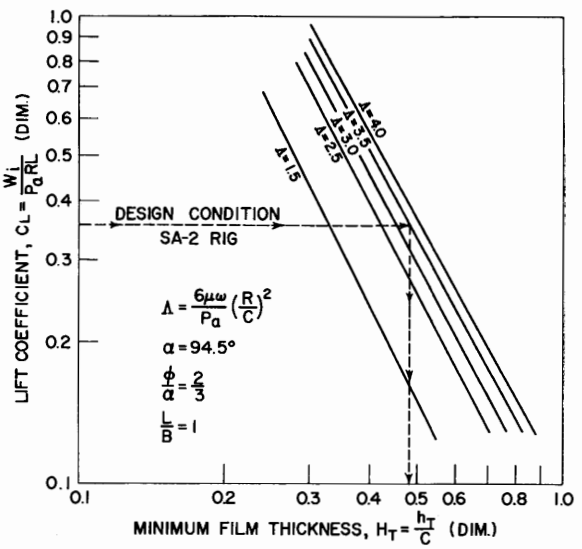

FIG. 5. Theoretical load coefficient C_L, versus minimum film thickness for various values of Λ.

plot indicated that an equation could be fitted to them. Such an equation was developed relating the basic performance parameters as shown in the following form:

$$W = \frac{P_a}{6}\left(\frac{C}{h_m}\right)^n \Lambda \frac{B^2}{(R/L)} f_a^2\,(R/L, \phi/\alpha, \Lambda) \qquad [11]$$

Equation [11] makes possible a direct comparison with the analytical results for flat sliders using incompressible lubricants. The incompressible case is equivalent to taking $n = 2$ in Eq. [11] and the side leakage factor f_a is a function only of the aspect ratio and pivot location.

The factor f_a was used by Raimondi and Boyd (*6*), and Muskat *et al.* (*5*). For the test conditions of speed and load encountered with the authors' gas-lubricated, tilting pad shoes, the f_a factor is a constant which is not speed dependent. This value was computed to be about 0.235 for $\phi/\alpha = \frac{2}{3}$, as compared to the values of $f_a = 0.245$ for the flat slider with an aspect ratio $L/B = 1$ as given by Raimondi and Boyd (*6*). Thus, it can be seen that one effect of compressibility is to slightly reduce the f_a factor with a corresponding reduction in load as compared to the incompressible case.

The other important variable of the above equation is the exponent "n" of the film thickness term. The value of "n" is slightly less than 2 for the compressible case and decreases slowly with increasing Λ. The value of "n" may be given by the expression:

$$n = 2.08 - 0.052\Lambda \qquad [12]$$

for Λ varying from 1.5 to 4.0.

Thus, the two theories predict that, for the same minimum film thickness, the compressible film will carry less load than the incompressible film with a flat slider.

Sample calculation

EXAMPLE I

An an illustration of the use of Eq. [11], the load-carrying capacity for a single pivoted pad will be computed from knowledge of the speed and minimum film thickness. The results will then be checked against the computer field map to test the accuracy of Eq. [11].

Assuming the following input data:

$R = 2.00$ inches
$C = 0.0015$ inch
$B = 3.3$ inches
$L = 3.3$ inches
$P_a = 14.7$ psia
$N = 17{,}650$ rpm
$\mu = 2.61 \times 10^{-9}$ reyns
$h_m = 0.0007$ inch
$\alpha = 94.5°$
$\phi/\alpha = \frac{2}{3}$

Then

$f_a = 0.235$
$\Lambda = 3.5$
$n = 2.08 - 0.052\,(3.5) = 1.898$

Equation (11) yields

$$W = \frac{14.7}{6}\left(\frac{C}{h_m}\right)^{1.898} \frac{(3.5)(3.3)^2(0.235)^2}{0.606}$$

$$= 8.51\left(\frac{C}{h_m}\right)^{1.898} = 36 \text{ lb}$$

(It is understood that a design pad load could have been specified for which the minimum operating film thickness h_m could have been calculated instead of specifying a film thickness and computing a load as in the example above.)

To check the results of Eq. [11] through the use of the computer field maps we can compute the load coefficient C_L, which equals $(W)/(P_a RL)$, to be

$$C_L = 36/(14.7)(2)(3.3) = 0.371$$

From this load coefficient and $\phi/\alpha = \frac{2}{3}$ the computer field map of Fig. 3 yields $\varepsilon = 0.59$ and $\xi = 60°$.

The corresponding leading (h_L) and trailing edge (h_T) film thicknesses are

$$h_L = C[1 + \varepsilon \cos \xi] = 0.00194 \qquad [13]$$

$$h_T = C[1 + \varepsilon \cos (\xi + \alpha)] = 0.000701 \qquad [14]$$

Since ξ is smaller than 85.5° the film thickness occurs at the trailing edge. The calculated value of h_T is in extremely good agreement with the one specified as a design parameter for this problem, thus confirming the good fit of Eq. [11] to the computer results.

Design of complete bearing

Figure 6 is obtained as a crossplot of the computer field map and is extremely useful in the design of complete bearings.

One of the crucial parameters governing the operation of a complete bearing is the setting of the pivot circle clearance c'. This is caused by the necessity for maintaining a stable hydrodynamic film under the top or preload shoe at very low speeds. With low speeds, the shaft will operate at very high eccentricity ratios with respect to the pivot circle setting, and the pivot film thickness of the top shoe may become larger than the machined-in radial shoe clearance.

If the top shoe should vibrate or be disturbed in any way from its equilibrium position when operating under the above conditions, the hydrodynamic restoring moment becomes negative, causing the shoe to rotate about its pivot until the leading edge of the shoe touches the shaft. In this "locked-in" position, the shoe forms a diverging fluid film clearance area which in turn creates a low pres-

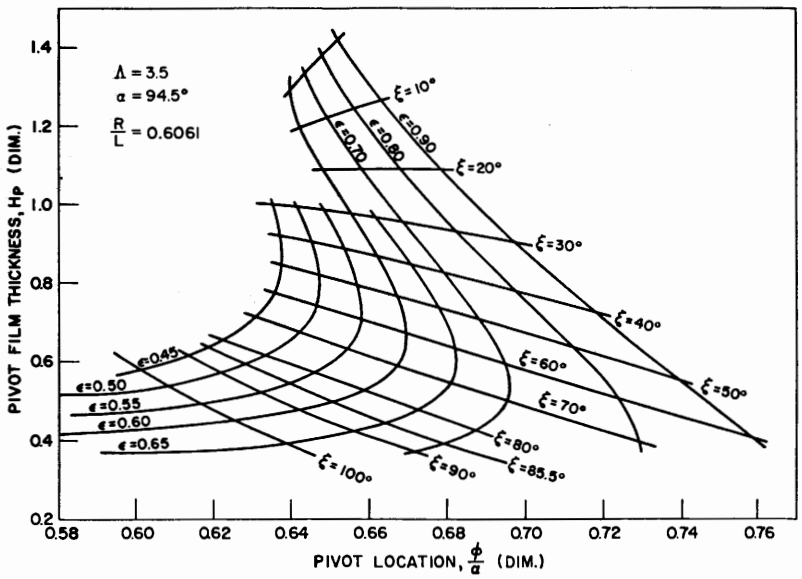

FIG. 6. Pivot film thickness versus pivot location for $\Lambda = 3.5$

sure region keeping the shoe in contact with the shaft (see Fig. 7).

To avoid this phenomenon, two recourses are available: one is to stabilize the shoe by the application of external moments and thus physically raise the leading edge and maintain the normal shoe attitude. It is this attitude that creates the load-carrying converging clearance space in the bearing. Second, by a proper choice of c'/C such that at the lowest predicted operating speed, a stable converging clearance is maintained under the top shoe. The proper choice of c'/C is dictated by the requirement that $h_{p3} < C$.

EXAMPLE II

As an illustration, a complete three-shoe bearing could be designed in the following manner:

Input data: Same individual shoe geometry as previous example.

Shaft weight = 86.5 lb

$$\beta = 50°$$
$$\Lambda = 3.5$$

Selecting a dimensionless pivot film thickness for the top shoe such that $h_{p3}/C < 1.0$ or assume $H_{p3} = 0.9$.

Figure 6 yields $\varepsilon = 0.65$ and $\xi = 36°$.

Entering the computer field map with these values, the top shoe load coefficient is determined to be $C_{L3} = 0.25$.

Then the load coefficient of the bottom shoes is:

$$C_{L1,2} = \frac{1}{2\cos\beta}\left[C_{L3} + \frac{W_s}{2P_aRL}\right] = 0.574 \qquad [15]$$

The computer field map (Fig. 3) gives the operating

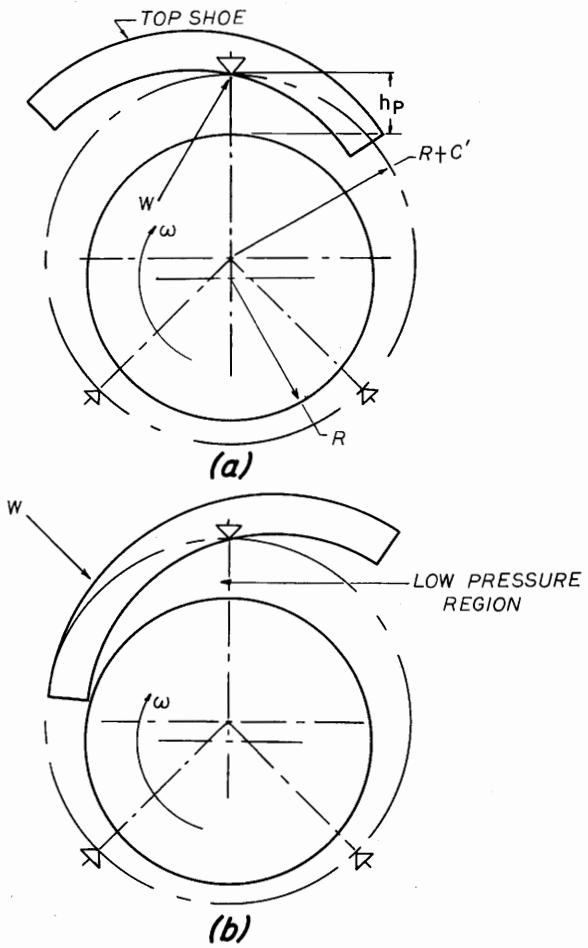

FIG. 7. Unstable shoe condition when (a) shoe position before "lock-up" and (b) shoe position at "Lock-Up."

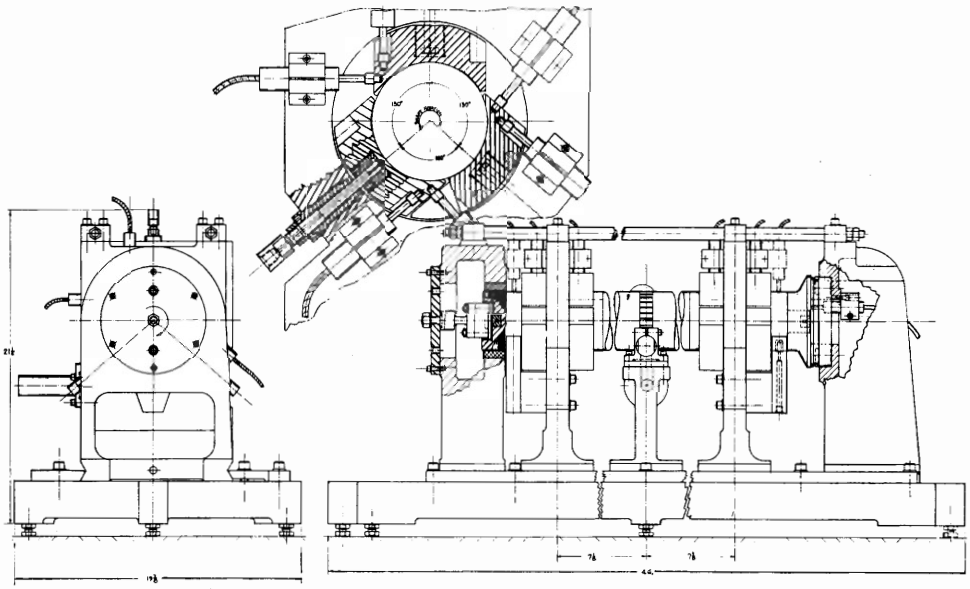

FIG. 8. Test rig with self-acting bearings, SA-2

conditions of the bottom pads as $\varepsilon_{1,2} = 0.62$ and $\xi_{1,2} = 77°$.

From Fig. 6, $H_{p1,2} = 0.53$.

The resulting pivot circle clearance is obtained from Eq. [1] rearranged as

$$\frac{C'}{C} = \frac{H_{p1} + H_{p2} + 2H_{p3}\cos\beta}{2[1 + \cos\beta]} = \frac{0.53 + 0.9 \times 0.643}{1.643} = 0.675 \quad [16]$$

Therefore

$$C' = 0.675 \times C = 1.012 \times 10^{-3} \text{ inches}$$

or the pivot circle radius should be approximately one mil larger than the shaft. The machined-in clearance C is of course $1\frac{1}{2}$ mils larger than the shaft.

Experimental investigation

The experimental rig is shown in Fig. 8. It consists of a plain cylindrical rotor driven by an air impulse turbine and supported by two symmetrically located three-pad bearings. The unit is provided with two externally pressurized lifters to independently support the shaft at low rotational speeds. At approximately 10,000 rpm the air supply to the lifters is shut off so that the total shaft load is carried hydrodynamically by the tilting-pad bearings. Capacitance probe mounts are provided so that the motion of the shaft and all shoes may be monitored with respect to ground. The film thickness is then obtained by differences. One shoe is also equipped with probes for the direct measurement of leading and trailing edge film thicknesses (Fig. 9). A close up of the bearing-shaft assembly without the top shoe is shown in Fig. 10.

Testing was performed without the top shoe in each bearing so that the bearing loads were due to shaft weight only and were thus accurately known. Under the above mentioned conditions the operating leading- and trailing-edge film thicknesses were measured and are shown in Fig. 11 along with a comparison of the theoretical predictions by the exact computer solution (*8*) and also Snell's approximation (*3*).

It will be remembered that Snell treated the pad surface as equivalent to a flat inclined slider and the fluid as being incompressible. As expected the latter assumption causes his solution to diverge from the exact one as the value of Λ increases. The deviation caused by the neglect of the sinusoidal variation of the clearance distribution (shoe curvature) will be considerable at high eccentricities.

The agreement between the computed and the experimental results is very satisfactory. Part of the small devia-

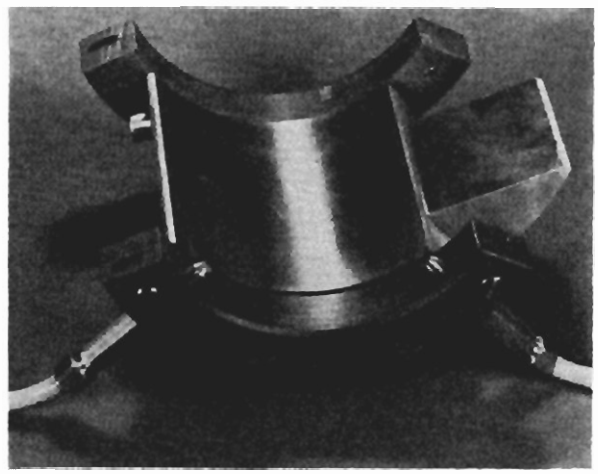

FIG. 9. SA-2 shoe with small probes attached

tion could be ascribed to squeeze film effects that are caused by the departure of the shaft surface from a perfect cylinder. Another source of error could be the uncertainty in the value of C, the machined-in shoe clearance, used in converting from ε and ξ to h_L and h_T. The original value of $C = 0.0015$ inch, employed in all calculations, is now probably slightly higher due to repolishing of the shaft surface.

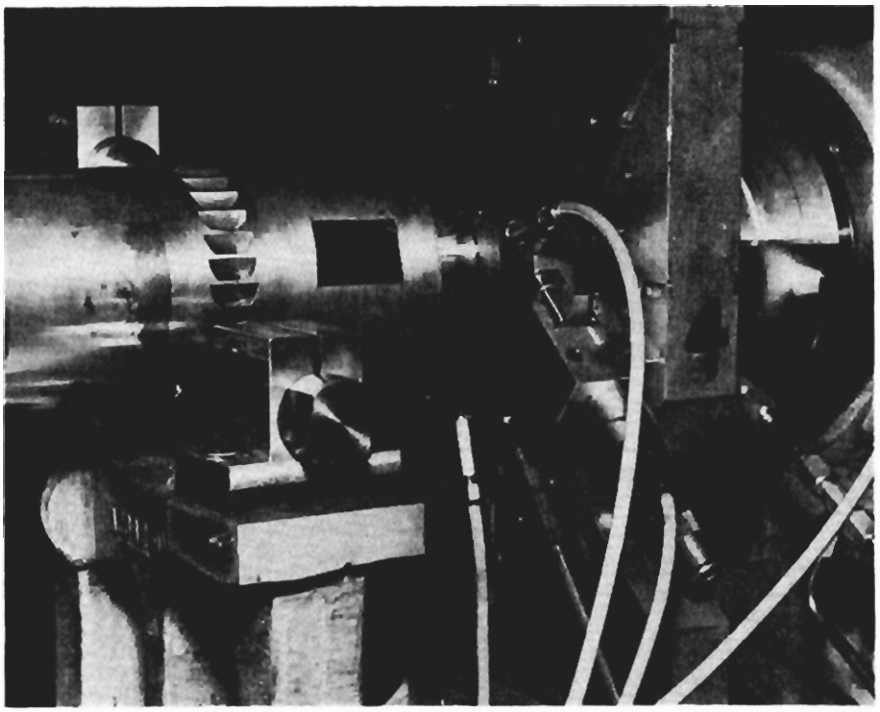

FIG. 10. SA-2 shoe installed on shaft

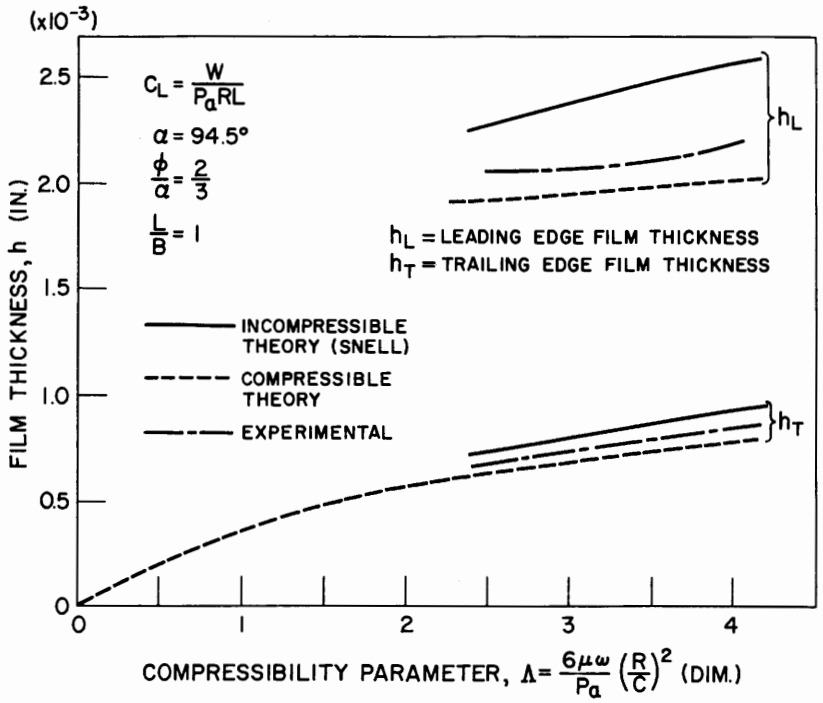

FIG. 11. Shoe film thickness measurements versus theoretical predictions

It was considered desirable to test the tilting-pad bearing at various pivot locations in order to experimentally ascertain the optimum pivot position.

In order to shift the effective pivot location, external moments were applied to the existing shoes. Whereas the resultant hydrodynamic force developed remains relatively unchanged, the location of the resultant load vector shifts from the physical pivot position to counteract the applied moment. This then is equivalent to having the shoe pivoted at a new position corresponding to the intersection of the shifted load vector with the bearing surface.

Figure 12 shows the effect of external moments on the leading and trailing edge film thicknesses and the corresponding effective pivot location. It can be seen that shifting the pivot location beyond the two thirds point toward the trailing edge of the pad causes a slight reduction in the trailing edge film thickness and a relatively large increase in the leading edge film thickness. In order to carry the equivalent load at increasing values of ϕ/α, the shoe inclination must increase, thus demonstrating that the optimum pivot location must be equal to or less than two thirds for the Λ condition of test. This is in agreement with the conclusions drawn by examining the computer field map, Fig. 3, which predicts values ranging from 0.62 to 0.65 depending upon speed and load. This *trend* is the same as for the flat slider bearing using an incompressible lubricant.

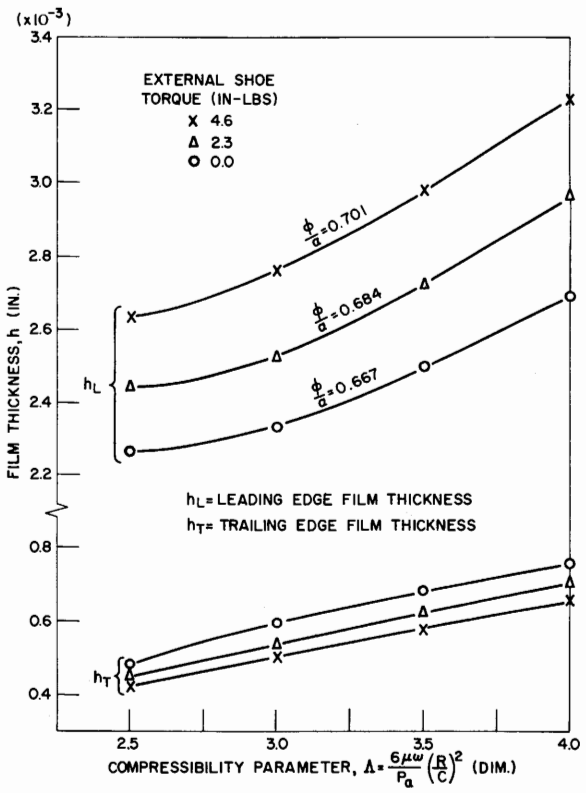

FIG. 12. Pivoted-pad film thicknesses versus Λ for various apparent pivot locations.

Conclusions

The good correlation obtained with the experimental results confirms the validity of the numerical computer solutions of Ref. (*7*). The usefulness of the field maps in the design of pivoted-pad gas bearings is enhanced by the establishment of a closed form equation which is applicable for the prediction of load-carrying capacity over a moderate range of the compressibility parameter Λ. The optimum pivot location has been determined to be in the range 0.62 to 0.65 for the range of Λ's investigated in contrast to the value of 0.5 previously proposed in Ref. (*3*).

ACKNOWLEDGMENT

The work reported herein was conducted under the sponsorship of the U.S. Atomic Energy Commission, under contract AT (30-1)-2512, Task 3 and the Office of Naval Research under contract Nonr-2432 (00), Task NR 061-113.

REFERENCES

1. FULLER, D. D., "General Review of Gas-Bearing Technology," Proceedings First International Symposium on Gas-Lubricated Bearings, Oct. 1959. U.S. Government Printing Office, A CR-49, pp. 1-29.
2. GROSS, W. A., "Gas Film Lubrication." Wiley, New York, 1962.
3. SNELL, L. N., "Pivoted-Pad Journal Bearings Lubricated by Gas," IGR-R/CA-285, 1958, United Kingdom Atomic Energy Authority, Industrial Group, 1958.
4. HAGG, A. C., "The Influence of Oil-Film Journal Bearings on the Stability of Rotating Machines," *J. Appl. Mech. ASME Trans.* **68**, A-211-220 (1946), Discussion, **69**, A77-A78 (1947).
5. MUSKAT, M., MORGAN, F., and MERES, W., "The Lubrication of Plane Sliders of Finite Width," *J. Appl. Phys.* **11**, 208 (1940).
6. RAIMONDI, A. A., and BOYD, J., "Applying Bearing Theory to the Analysis and Design of Pad-Type Bearings," *ASME Trans.* **77**, 287 (1955).
7. CASTELLI, V., STEVENSON, C. H., and GUNTER, E. J., "Steady-State Characteristics of Gas-Lubricated, Self-Acting, Partial-Arc, Journal Bearings of Finite Width," Interim Report I-A2049-18, April 1963, The Franklin Institute.
8a. FULLER, D. D., EUSEPI, M. W., and GUNTER, E. J., "The Application of Gas-Lubricated Bearings to High Speed Turbo-Machinery," Quarterly Technical Report Q-A2392-3-5, Franklin Institute, prepared for AEC under Contract No. AT(30-1)-2512, Mod. No. 3, 1962.
b. GUNTER, E. J., HINKLE, J. G., and FULLER, D. D., "The Application of Gas-Lubricated Bearings to High Speed Turbo-Machinery," Quarterly Technical Report Q-A2392-3-6, Franklin Institute, prepared for AEC under Contract No. AT(30-1)-2512, Mod. No. 3, 1962.
c. GUNTER, E. J., HINKLE, J. G., and FULLER, D. D., "The Application of Gas-Lubricated Bearings to High Speed Turbo-Machinery," Quarterly Technical Report Q-A2392-3-7, Franklin Institute, prepared for AEC under Contract No. AT(30-1)-2512, Mod. No. 3, 1962.
9. GUNTER, E. J., and FULLER, D. D., "Recent Progress on the Development of Gas-Lubricated Bearings for High Speed Rotating Machinery," USAF Fluids and Lubricants Conference, April, 1963.

Appendix

Derivation of Pivot Circle Clearance

For a three-pad bearing configuration the shoe pivot points form a unique circle referred to as the pivot circle. An important design parameter is the value of C', the pivot circle clearance setting. To completely specify the orientation of the journal with respect to the pivot circle three quantities must be known. These quantities are:

(a) $R + C' =$ pivot circle radius
(b) $e' =$ pivot circle eccentricity
(c) $\theta' =$ attitude angle

The above quantities will be expressed in terms of the shoe pivot film thicknesses h_{pi}.

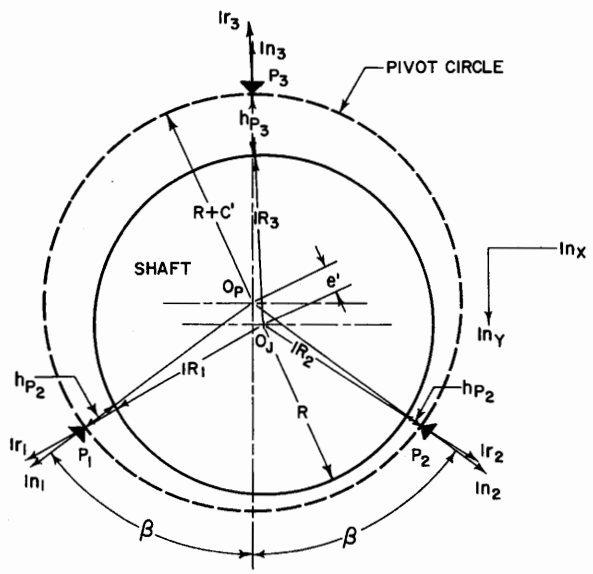

Fig. 13. Pivot circle and shaft geometry

From Fig. 13 it can be seen that the position vectors from the pivot circle center O_p to the shoe pivot points P_i $(i = 1, 2, 3)$ can be expressed as

$$\vec{o_pP^{P_i}} = (R + C')\,|n_i\,;\ i = 1,2,3 \qquad [17]$$

where

$|n_i =$ unit vector set directed from O_p to P_i; $i = 1,2,3$

The above position vectors can also be expressed as

$$\begin{aligned}\vec{o_pP^{P_i}} &= \vec{o_pO_j} + \vec{o_jP^{P_i}} \\ &= \vec{e'} + \vec{R_i} + \vec{h_{pi}} \\ &= \vec{e'} + (R + h_{pi})|r_i\,;\ i = 1,2,3 \end{aligned} \qquad [18]$$

where

$|r_i =$ unit vector set directed from O_j to P_i; $i = 1,2,3$

$\vec{e'} =$ eccentricity vector $= x\,|n_y + y\,|n_y$

$|n_x, |n_y =$ orthogonal cartesian unit vectors

Equating the two sets of position vectors

$$(R + C')\,|n_i = x\,|n_x + y\,|n_y + (R + h_{pi})|r_i \qquad [19]$$

The equations of transformation between the $|n_i$ unit vector set and the orthogonal cartesian unit vectors is given by

$$\begin{bmatrix} |n_1 \\ |n_2 \\ |n_3 \end{bmatrix} = \begin{bmatrix} -\sin\beta & \cos\beta \\ \sin\beta & \cos\beta \\ 0 & -1 \end{bmatrix} \begin{bmatrix} |n_x \\ |n_y \end{bmatrix} \qquad [20]$$

Take the dot product of Eq. [19] by the unit vectors $|n_i$

$$[(R + C')\,|n_i = x\,|n_x + y\,|n_y + (R + h_{pi})\,|r_i] \cdot |n_i \qquad [21]$$

$i = 1,2,3$
if $e'/R << 1$ then
$|r_i \cdot |n_i$ or $|r_1 \cdot |n_1 = |r_2 \cdot |n_2 = |r_3 \cdot |n_3 \approx 1$

The above results in three scalar equations which are

$$\begin{aligned} &\text{(a) } R + C' = x\sin\beta + y\cos\beta + h_{p1} + R\ ;\ i = 1 \\ &\text{(b) } R + C' = x\sin\beta + y\cos\beta + h_{p2} + R\ ;\ i = 2 \\ &\text{(c) } R + C' = -y + h_{p3} + R\ ;\ i = 3 \end{aligned} \qquad [22]$$

Solving for C'

$$C' = \frac{h_{p1} + h_{p2} + 2\cos\beta\, h_{p3}}{2[1 + \cos\beta]} \qquad [23]$$

Solving for y

$$y = h_{p3} - C' = \frac{2h_{p3} - (h_{p1} - h_{p2})}{2[1 + \cos\beta]} \qquad [24]$$

[22.c]

Solving for x

$$x = \frac{h_{p1} - h_{p2}}{2\sin\beta} \qquad [25]$$

Solving for the attitude angle θ' of the journal center with respect to the pivot circle

$$\begin{aligned}\theta' &= \tan^{-1}\frac{y}{x} \\ &= \tan^{-1}\left[\left(\frac{\sin\beta}{1 + \cos\beta}\right)\left(\frac{2h_{p3} - (h_{p1} + h_{p2})}{h_{p1} - h_{p2}}\right)\right] \end{aligned} \qquad [26]$$

DISCUSSION

A. A. RAIMONDI (*Westinghouse Research Lab, Pittsburgh 35, Pennsylvania*):

A pivoted pad journal bearing with only three pads would ostensibly have an undesirable characteristic, particularly for a gas bearing. The variation in eccentricity with the direction of the load (between the pads as compared say to "on" the pivot) is appreciable resulting possibly in large changes in stiffness. This effect is mitigated as the number of pads is increased (see Ref. *A1*). It would seem that at least four and preferably six or more should be used. Viewed in this light, the effect of pad curvature is lessened as the number of pads increases (since the pad arcs become considerably shorter) so that flat pad theory should give better agreement. The agreement for the present case appears to the writer to be tolerable and might have been better had compressibility been accounted for.

The treatments of pivoted pad journal bearings available presently are not necessarily restricted to flat pad approximations. Reference (*A2*) points out that curvature is important and accounts for curvature by using a crowned pad technique.

The subject of lock-up has already been treated in some detail and brought to attention in a recent paper (*A2*). There it is called "spragging" and means of controlling it shown. The top (unloaded) pad of a three pad bearing would be almost certain to sprag.

Spragging can be a real problem in gas bearings and we have found that when the unloaded pad does sprag, it can interfere with the proper operation of the loaded pad(s).

REFERENCES

A1. BOYD, J., and RAIMONDI, A. A., "An Analysis of the Pivoted-Pad Journal Bearing," *Mech. Eng.* May, 380-386 (1953).

A2. BOYD, J., and RAIMONDI, A. A., "Clearance Considerations in Pivoted-Pad Journal Bearings," *ASLE Trans.* **5**, 418-426 (1962).

P. C. WARNER (*Mechanical Technology, Inc., Latham, N. Y.*):

The authors' interesting paper and invaluable data will be particularly appreciated by those designers of high-speed rotating equipment who are faced with the most difficult gas-lubricated journal bearing design problems. In view of the strong assets of the tilting pad type of bearing and its widespread use where conventional lubricants are employed, it is difficult to understand the almost complete lack of theoretical treatment accorded it. Fortunately, the authors' paper goes a long way toward filling the obvious gap.

Inasmuch as the chief reason for employing this pad type of bearing is to eliminate fluid film whirl, it would appear that perhaps less attention should be spent on the precise details of minimum film thickness and other similar quantities and more on that property which makes a properly designed pad bearing unable to support fluid film whirl. In Hagg's analysis (*4*), which visualized incompressible lubricants, and perhaps is restricted to reasonably small Λ values, the salient point would appear to this discussor to be the statement that, "Because the bearing pad is pivoted and free to rotate, not only is the direction of P from pivot point to journal center, but the magnitude of P is a single valued function of the distance separating the pivot center and journal center." Certainly if pad inertia is so great that the pads cannot follow the vibrating shaft, then the pads are not free to rotate, and the force need not go through the pad pivot point; hence, the stability properties of the bearing must degenerate to those of fixed partial arc bearings. While adequate film thickness at each pad is certainly a necessary condition for proper bearing design, it is not sufficient in most cases, and several design decisions should take cognizance of the extreme desirability of low inertia pads and high angular stiffness of the lubricant film. It is felt by this discussor that it is very desirable to keep the pitching and rolling natural frequencies of all the pads at least twice as high as operating speed. Such an accomplishment assures proper ability of the pads to track the journal, hence freedom from fluid film whirl.

Further, the fluid film properties required to estimate the pitching and rolling frequencies can be calculated by numerical differentiation of the computer map, Fig. 3, provided that the frequency of motion involved isn't too high.

AUTHORS' CLOSURE:

Mr. Raimondi, in his discussion, points out that a three-pad bearing arrangement would have an appreciable variation in bearing stiffness in transverse directions. This is true and has been experimentally observed. One aspect of the experimental phase of the pivoted-pad gas bearing investigation has been to obtain quasi-static bearing stiffness values at various speeds. These values have been obtained from load-deflection data obtained by a foil bearing device which preloads the shaft by various amounts. The difference in bearing stiffness characteristics has manifested itself in the behavior of the rotor rigid body resonance frequencies ("critical speeds"). Several resonance frequencies are monitored on the oscilloscope in which the rotor motion is predominantly a horizontal mode at low speed and changes to essentially a vertical mode at higher speeds. All resonance frequencies encountered occur well below the design speed of 18,000 rpm for the unit, in the 5000–10,000 rpm range. No difficulty has ever been encountered in passing through these resonance speeds, and as such the authors feel that unsymmetrical bearing stiffness in itself will not preclude the successful operation of a three-pad gas-lubricated bearing arrangement.

Of paramount importance, however, to the successful operation of a gas bearing rotor of this size, is the high degree of rotor balancing that must be attained. Since the viscosity of air is very low, approximately 1/1000 that of oil, the damping characteristic of a gas-lubricated bearing is substantially lower than that obtained with a conventional oil-lubricated bearing. As such, in order to maintain permissible amplitudes of motion while passing through the rotor resonance frequencies, the rotor must be extremely well balanced. Considerable difficulty was encountered in trying to obtain the necessary rotor balance by commercial techniques. A method was finally devised whereby the rotor was accurately and rapidly balanced in place by monitoring the rotor motion by means of the capacitance probes (*8b*, *9*).

It was felt that the three-pad bearing arrangement is preferable because this configuration yields the maximum load-carrying capacity and also for the consideration of aligning the shoes. For a three-pad arrangement the three pivot points will determine a unique pivot circle setting. If more than three shoes were employed, it was felt that some difficulty might be encountered in trying to align the shoes so that the pivots would fall on a common pivot circle.

The authors wish to iterate here that the analysis does include the effect of compressibility of the lubricant as well as shoe curvature since the developed computer program takes into considera-

tion the exact film distribution between the shaft and the shoe. Hence Eq. [11] presented in the text includes the effects of shoe curvature as well as lubricant compressibility. The film distribution corresponding to the above case is not linear (shoe arc length = 94.5°) but is a slowly varying sinusoidal function. As Mr. Raimondi mentions, the use of more shoes (reduction in shoe arc length) will reduce pad curvature and hence the shoes will be better approximated by flat slider theory.

The authors appreciate the viewpoint taken by Mr. Warner in that it would be desirable to have more information regarding the stability characteristics of the pivoted-pad bearing arrangement. It is because of the highly stable characteristics with respect to half-frequency whirl that this system has been so intensively investigated. The main purpose of this paper, however, has been to present some of the steady-state characteristics of the pivoted pad bearing such as shoe load capacity, minimum film thickness, and optimum shoe pivot location. The authors hope at a later date to present information on such system dynamic characteristics as half-frequency whirl, shoe flutter, and rotor resonance frequencies.

There are several operating characteristics that the authors wish to comment on at this time. One is the possible occurrence of shoe flutter with tilting-pad shoes. As Mr. Warner has stated, it seems desirable to construct the pads with low moments of inertia so as to keep the pad rolling and pitching flutter frequencies well above the operating speed of the unit. In the design of the authors' unit, the self-acting shoes were designed with large inertia properties in order to obtain accurate film thickness data. The natural shoe flutter frequency in the direction of motion appears to be less than one-half of the design speed of the unit, i.e., 18,000 rpm. No operating difficulties have ever been encountered due to shoe motion.

Another factor which seems to have a strong influence on the dynamic behavior of a tilting-pad gas-lubricated bearing system is the design of the shoe pivots.

Several different sets of pivots have been used in the testing and have resulted in a considerable variation in both shoe and rotor performance. One set of pivots employed had a cone and socket design which permitted an accurate alignment of the shoe with respect to the shaft for precise film thickness measurements. With this type of pivot, an unstable rotor orbit was monitored in which half-frequency whirl appeared to be present. This phenomena occurred with two different sets of shoes having different aspect ratios. In both cases, the apparent half-frequency rotor orbits occurred at a speed of approximately twice the rotor translatory resonance frequency. It was felt that sufficient friction present in this pivot design could have caused the shoes to behave more as fixed partial arc bearings rather than as pivoted pad bearings. When a second pivot design of a crown pivot on a flat bushing was employed, the unstable whirl orbiting was eliminated, but the observed shoe motion was three times the previous value. This might indicate that some external damping in a pivoted pad shoe is desirable to limit shoe motion but not so much as to cause the bearing to behave as a fixed pad and hence induce whirling.